Structure, Bonding, and Lowest Energy Transitions in Unsymmetrical Squaraines: A Computational Study[§]

K. Yesudas,[†] **G. Krishna Chaitanya,**[†] **Ch. Prabhakar,**[†,‡] **K. Bhanuprakash,***[,†] **and V. Jayathirtha Rao***[,‡]

Inorganic Chemistry Division and Organic Chemistry Division, Indian Institute of Chemical Technology, Hyderabad-500 007, India

Natural resonance theory (NRT) and natural bond orbital (NBO) analysis have been carried out on a simple symmetrical and an unsymmetrical substituted squaraine with a view of understanding the structure of the latter type of squaraines. It is found that there are some fundamental differences in the structure and bonding between these two types of squaraines particularly in the resonance weights and delocalization energies. These differences are expected to reflect in the low energy transitions and charge transfer in these squaraines. To investigate this, the nature of the lowest energy transitions occurring on excitation in unsymmetrical squaraines has been studied using high-level symmetry adapted cluster−configuration interaction method (SAC/SAC−CI) and compared with reported experimental observations. In general the agreement with the experimental data is very good. The transition dipole moment always lies on the π-backbone and is quite large in magnitude. The ground state dipole moment in some cases does not change in the excited state upon excitation while in some other cases there is a large reduction/enhancement in the magnitude indicative of some charge rearrangement in this direction. Inclusion of the solvent using the IEFPCM model, a slightly better agreement with the experiment is found in some cases. Studies are carried out with a different basis set and it is found that the change in basis set has very little effect on the transition energies. In the case of weak side donor groups attached to the central ring the larger charge transfer to the central acceptor ring in general takes place from the O^- atoms of the squarylium moiety while in the case of strong donors the charge transfer from the O^- atoms to the central rings drop down. We have not observed any correlation between the charge transfer in the excited state to the central ring from the side donor groups and the lowest energy excitation in the molecules. Reduction of the HOMO−LUMO gap (an indication of increase of the diradicaloid character) always leads to a bathochromic shift.

Introduction

Diradicaloid molecules are obtained by lowering the diradical nature of a diradical through substitution.[1] These are characterized by the presence of nearly degenerate frontier molecular orbitals, which are occupied by two electrons. An example is shown in Scheme 1. In the left side of the scheme an unsubstituted diradical is shown whose highest occupied orbitals are singly occupied and are degenerate. We have indicated in the scheme that it could be either a triplet or a singlet diradical. This diradical can be modified to a simple squaraine (SQ) by substitution as shown in the same scheme. We calculate the lowest singlet and triplet energies of this substituted squaraine using the DFT-B3LYP/6-31G(d,p) method.[2] The HOMO−LUMO gap (HLG) lies around 9.73 eV in the singlet molecule while the singlet -triplet energy gap ($\Delta E(S_0-T_1)$), with the singlet having lower energy, is around 52.2 kcal/mol. The λ_{max} of absorption is calculated by the SAC−CI method to be around 288 nm while the experimental determined value is 285 nm.[2,3] This example shows the lowering of the diradical nature upon substitution. With increase in the π-electron density in the substitution there is a lowering of the HLG to 5.24 eV in the

third molecule as seen in the same scheme. This lowered HLG could be due to both increase in conjugation and an increase in the diradical nature (a diradicaloid). Here it is also clearly seen that there is a decrease in the singlet−triplet energy gap. Thus, the $\Delta E(S_0-T_1)$ gap is lowered from 52.2 kcal/mol in the simple substituted squaraine to 13 kcal/mol, but the singlet system is still lower in energy.[2] The λ_{max} of absorption calculated by the SAC−CI method is the same as the experimental determined value of 805 nm.[2,4] According to Wirz one criterion to classify a molecule as a diradicaloid is the energy of the singlet−triplet splitting which should lie around 10−100 kJ/mol.[1,5] The $\Delta E(S_0-T_1)$ energy of the third molecule in the scheme lies within this range. Another criterion would be the occupation numbers of the natural orbitals (vide infra).[1] Further comparison of the frontier molecular orbitals (HOMO and LUMO) of the third molecule reveal substantial differences in the electron density in the central oxyallyl ring and not much in the extended π-conjugation, indicating a more diradicaloid character.[2,6] Some of these SQ molecules are known to absorb in the near-infrared region (NIR) and hence are also referred to as NIR dyes in general.[1,7−9]

SQ dyes are novel class of organic dyes that play a crucial role in the development of various types of materials for the applications such as nonlinear optics, electrophotography, xerography, photovoltaics, chemo sensors, biological labeling,
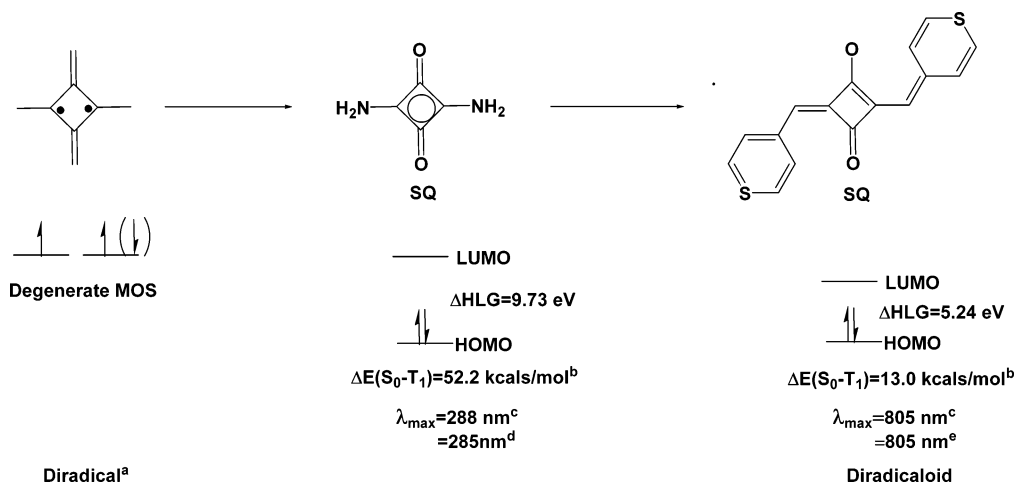
* Corresponding author. E-Mail: bhanu2505@yahoo.co.in.
[†] Inorganic Chemistry Division, Indian Institute of Chemical Technology.
[‡] Organic Chemistry Division, Indian Institute of Chemical Technology.

SCHEME 1

^{a} Diradical could be either a singlet or triplet as indicated in parentheses. ^{b}Calculated at B3LYP/6-31G(d,p) level. Reference 2. ^{c}Calculated using SAC/SAC−CI. Reference 2. ^{d,e}Experimentally obtained. References 3 and 4.

and photodynamic therapy.[7−9] There has been a lot of interest in these molecules in the very recent times due to these varied applications. The conventional representation of SQ dyes is as a donor−acceptor−donor (D−A−D) type of structural arrangement. In general, this type of structural arrangement is known as symmetrical SQ dye derivatives, and it is assumed that the charge transition takes place from the two side donor groups (aromatic moieties) to the central super acceptor (C_4O_2 ring) part.[10] Many studies with a change in the donor group to improve the absorption properties have been reported.[11−16] It is believed that increasing the donating capacity of the side groups would red-shift the absorption.[7−9] This also lead to the synthesis of many unsymmetrical SQ dye derivatives (D−A−D′).[17−22] High-level theoretical studies of the symmetric squaraines have been reported earlier which give us some idea of the structure, bonding and transitions in these molecules, but for the unsymmetrical cases we have not come across any such detailed studies.[2,10,23]

NBO and NRT Analysis of Substituted Symmetrical and Unsymmetrical Squaraines

An analysis of the bonding in these molecules and estimation of the contribution of the localized orbitals or rather the covalent nature should help us to understand the properties. One way of studying this contribution is through natural bond orbital (NBO) analysis introduced by Weinhold and co-workers.[24] The NBO theory provides the orthogonalized and linearized basis sets for the one center (core and valence lone pairs), two center (Bonding and antibonding), three center four electron (if possible) and Rydberg type of molecular orbitals based on the occupation of the electrons in that corresponding orbital (The antibonding orbitals we talk about here have some nonzero occupancy and are not the same as the virtual orbitals of the MO theory[25]). The additional advantage comes from this NBO approach as it mimics the localized Lewis type of molecular orbital pictures and corresponding localized bonds. Even the small residual energy values and charge contributions in the saturated systems are due to the delocalization and noncovalent interactions. The NBO program makes it possible to determine the energetic effect of deleting certain NBOs, groups of NBOs, or specific NBO donor−acceptor interactions. The delocalization energy or the non-Lewis energy (E_{nl}) is then estimated by deleting all the

antibonding and the Rydberg orbitals from the calculations and forcing the electrons to occupy the localized or the Lewis orbitals.

In addition, this noncovalence or hyper conjugated interactions can be further examined at the orbital level by NBO method as the second order correction to interaction energy $E(2)$ between the occupied molecular orbitals (donor, i) and the neighboring unoccupied molecular orbitals (acceptor, j). This interaction energy represents the charge delocalization due to the loss of electronic occupation from the localized Lewis molecular orbital to the non- Lewis molecular orbital leading to the distribution of electronic charge and thus the perturbation from idealized Lewis structure description. The interaction energy (stabilization energy) $E(2)$ associated with the delocalization occurred ($2e^-$ stabilization) between the donor NBO (i) and the acceptor NBO (j) can be estimated from eq 1.

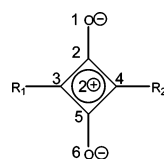$$E(2) = \Delta E_{ij} = q_i/[F(i, j)^2 (E_j - E_i)] \tag{1}$$

where q_i is the donor orbital occupancy, E_i and E_j are the diagonal elements (orbital energies) and $F(i, j)$ is the off-diagonal NBO Fock matrix element.

Thus, to understand the nature of bonding interactions and occupations we have carried out NBOanalysis incorporated in G03W using the B3LYP/6-31G(d,p) optimized geometries of the simple substituted squaraines—both symmetrical and unsymmetrical.[26] The example chosen for the symmetric squaraine is the 3,4-NH_2 substituted one, while for the unsymmetrical case, one of the NH_2's is replaced by the OH group (shown in Table 1). The geometries have been optimized using the B3LYP/6-31G(d,p) method. Only the lowest singlet is calculated. The NBO analysis is then carried out on these geometries. The % of Lewis character obtained is 95.5% for the symmetric case and 96.64% for the unsymmetrical case. This indicates fairly high electron delocalization in both cases.

The results of the second-order perturbation calculations are shown in Table 1a, for the simple symmetric case (in parentheses) and for the unsymmetrical case. In the symmetrical squaraine the large interactions are due to the lone pair of electrons on the oxygen atoms interacting with the antibonding orbitals (non Lewis orbitals) of the ring. The interaction energy is around 23.3 kcal/mol and is equal in magnitude for all the interactions due to symmetry. The non-Lewis energy obtained

Unsymmetrical Squaraines

J. Phys. Chem. A, Vol. 110, No. 41, 2006 **11719**

TABLE 1: (a) Second Order Perturbation Energy ($E^{(2)}$, kcal/mol) Analysis of the Symmetrical and Unsymmetrical Squaraines (Where Only Important Interactions Involving Lone Pairs of the Central Moiety Are Presented Below)[a] and (b) Important NBO Occupancies Obtained Using a Non-Zwitterionic Structure as the Default Input[a]
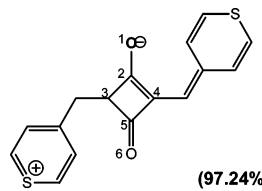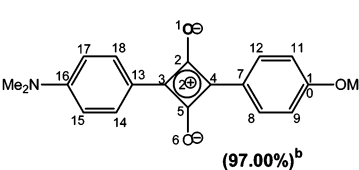
(a)

For Symmetric molecule $R_1=R_2=NH_2$ **(95.50%)[b]**
For Unsymmetric molecule $R_1=NH_2$, $R_2=OH$ **(96.64%)[b]**

donor	occupancy (e)[c]	acceptor	occupancy (e)[c]	$E^{(2)c}$
n_{O1}	1.84039 (1.84656)	σ^*_{C2-C3}	0.09006 (0.08265)	25.18 (23.28)
n_{O1}	1.84039 (1.84656)	σ^*_{C2-C4}	0.09023 (0.08265)	23.67 (23.28)
n_{C4}	0.90656	$\pi^*_{O1=C2}$	0.39053	60.39
n_{C4}	0.90656	$\pi^*_{C5=O6}$	0.42378	67.40
n_{O6}	1.84350 (1.84656)	σ^*_{C3-C5}	0.08912 (0.08265)	24.54 (23.28)
n_{O6}	1.84350 (1.84656)	σ^*_{C4-C5}	0.08915 (0.08265)	22.35 (23.28)

(b)

(97.24%)[b]   **(97.00%)[b]**

Molecule-A   **Molecule-B**

	molecule A			molecule B	
NBO	occupancy (e)			NBO	occupancy (e)
π_{O1-C2}	1.98480			π_{O1-C2}	1.98598
π_{C5-O6}	1.98480			π_{C5-O6}	1.98600
n_{O1}	1.84988			$\pi_{C14-C15}$	1.73930
n_{C4}	0.95475			$\pi_{C17-C18}$	1.73964
n_{O6}	1.84988			n_{O1}	1.85841
n^*_{C3}	0.95475			n_{O6}	1.85806
π^*_{O1-C2}	0.34411			n_{C16}	0.93295
σ^*_{C2-C3}	0.06828			n^*_{C4}	0.89879
σ^*_{C2-C4}	0.07745			σ^*_{C2-C3}	0.07341
σ^*_{C3-C5}	0.07745			σ^*_{C2-C4}	0.07144
σ^*_{C4-C5}	0.06828			σ^*_{C3-C5}	0.07378
π^*_{C5-O6}	0.34411			σ^*_{C4-C5}	0.07174
				$\pi^*_{C14-C15}$	0.25467
				$\pi^*_{C17-C18}$	0.25473

[a] The asterisk represents a non Lewis orbital. [b] The % of Lewis structure is given in parentheses. [c] For symmetrical SQ values are shown in parentheses.

by deleting all the antibonding orbitals and Rydberg orbitals in the occupation is around 847 kcal/mol. In the unsymmetrical case one notices that the lone pair (LP) of oxygens have almost similar interaction energy with the orbitals of the ring. But an extra interaction energy of the LP of one carbon (with one occupied electron) in the ring with the non-Lewis C=O bond is also seen and this is quite large, i.e., 60 and 67 kcal/mol. Here the non-Lewis energy is around 769 kcal/mol.

NBO analysis of larger molecules is also carried out. The molecules are indicated in the same table (Table 1b). Here it is slightly complicated. Too many resonance structures are possible. An initial choices of zwitterionic structures using CHOOSE option yields occupations for a charge separated states with equally large Lewis contribution. Default option (a nonzwitterionic character) is chosen here. The diradicaloid nature of the symmetric case is seen with occupation of one electron in the LP orbital of C4 and another electron in the LP* orbital of C3. In the unsymmetrical case the LP* occupation of C4 is 0.9e while the second electron occupies C16 LP, which is on the phenyl ring. The % of Lewis character obtained is around 97% for both symmetrical and unsymmetrical SQ molecules. The

occupation of LP* is not commonly observed and may represent an excited-state configuration.[25] We do not elaborate on this further. Instead we make use of the results of the smaller molecules and the $\Delta E(S_0-T_1)$ to emphasize the diradicaloid character.

To understand the ground state structure and resonance, we have applied the recently suggested natural resonance theory (NRT) method. NRT provides an analysis of the electron density, obtained by MO ab initio programs in terms of resonance structures and weights.[27] The one electron reduced density operator, Γ, is expanded in terms of Γ_α, which represents the corresponding reduced density operator of an idealized resonance structure. In other words

$$\Gamma = \sum_\alpha W_\alpha \Gamma_\alpha \qquad (2)$$

where the weights, W_α are constrained to satisfy

$$W_\alpha \geq 0, \sum_\alpha W_\alpha = 1$$

TABLE 2: Summary of NRT Analysis for Symmetrical and Unsymmetrical Squaraines, Showing Leading Resonance Structure Weight (wα$_i$ with Degeneracies (Deg), Bond Orders, and Atomic Valencies with Covalent and Ionic Electrovalent Contributions and Non-Lewis Energy (E_{NL})^a
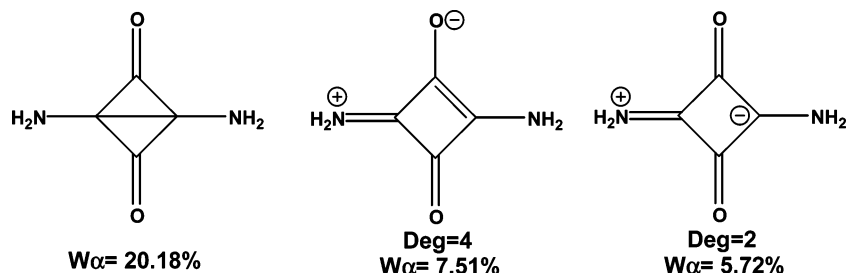
	NRT bond order				NRT valency			
bond	total	covalent	ionic	atom	total	covalent	ionic	E_{NL} (kcal/mol)
O−C	1.8578	1.1931	0.6647	O	1.8957	1.1931	0.7026	847.17
C−C	1.0555	0.8991	0.1564	C	3.9687	2.9912	0.9775	
				C	3.7155	2.7811	0.9344	
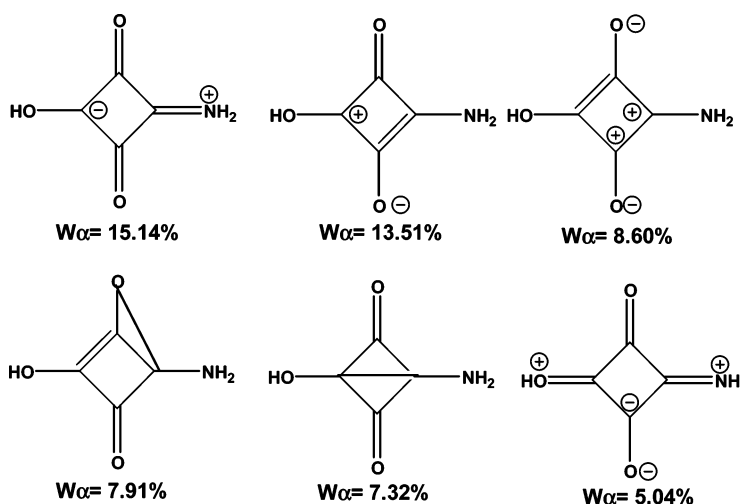
	NRT bond order				NRT valency			
bond	total	covalent	ionic	atom	total	covalent	ionic	E_{NL} (kcal/mol)
O1−C2	1.8818	1.2194	0.6624	O1	1.9609	1.2985	0.6624	769.00
C2−C3	0.9384	0.7910	0.1473	C2	3.9587	2.9377	1.0210	
C2−C4	1.1385	0.9273	0.2112	C3	3.8350	2.8897	0.9454	
C3−C5	1.0779	0.8918	0.1862	C4	3.5837	2.8274	0.7563	
C4−C5	1.1640	1.1026	0.0614	C5	3.8307	3.0072	0.8235	
C5−O6	1.5888	1.0128	0.5760	O6	1.6477	1.0136	0.6341	

^{a} For numbering please refer to Table 1.

For the weak delocalization NRT analysis is carried out with a single reference structure and on the other hand for the strong delocalization multireference NRT analysis is carried out.[27]

Our NRT calculations on larger SQ molecules yielded too many resonance structures with weights less than 2%. These cannot be meaningfully discussed. Hence we carry out the NRT calculations on the two simple symmetric and unsymmetrical squaraines at the B3LYP/6-31G(d, p) obtained geometry using the GENNBO code.[28] We first generate the FILE47 from the G03W program for this run. We use the default algorithm for generating the resonance structures.[25] Thus, those structures which contribute more than 35% weight and have threshold energy of more than 1.0 kcal/mol are only selected. The results of the NRT study are given in Table 2. The weight of the leading nondegenerate resonance structure is 20%. This has a formal long bond inside the ring. The charge-separated structures contribute around 28% with the negative charge on the oxygen

atom and the positive charge on the nitrogen. Another charge-separated structure is contributing around 10% with the positive charge on the nitrogen atom and this time the negative charge inside the ring. This has a degeneracy of 2. The results of the unsymmetric case are also shown in the same table. Here we notice that there is a drop in the long bond structure and it has a weight of only 7%. On the other hand another long bond structure crops up with the oxygen atom and it has a contribution of 7.9%. There are a larger number of charge-separated structures. Structure with negative charges on both the oxygens and the two positive charges inside the ring structure has a weight of 8.6%. The long formal bonds in the above examples could be representative of small diradicaloid character.

The bond order and valencies are also shown in the same table. It is clearly seen there is a reduction in the bond order in the case of one C−O bond in the unsymmetrical squaraines. From the valency it is also clear that one of the oxygen atoms
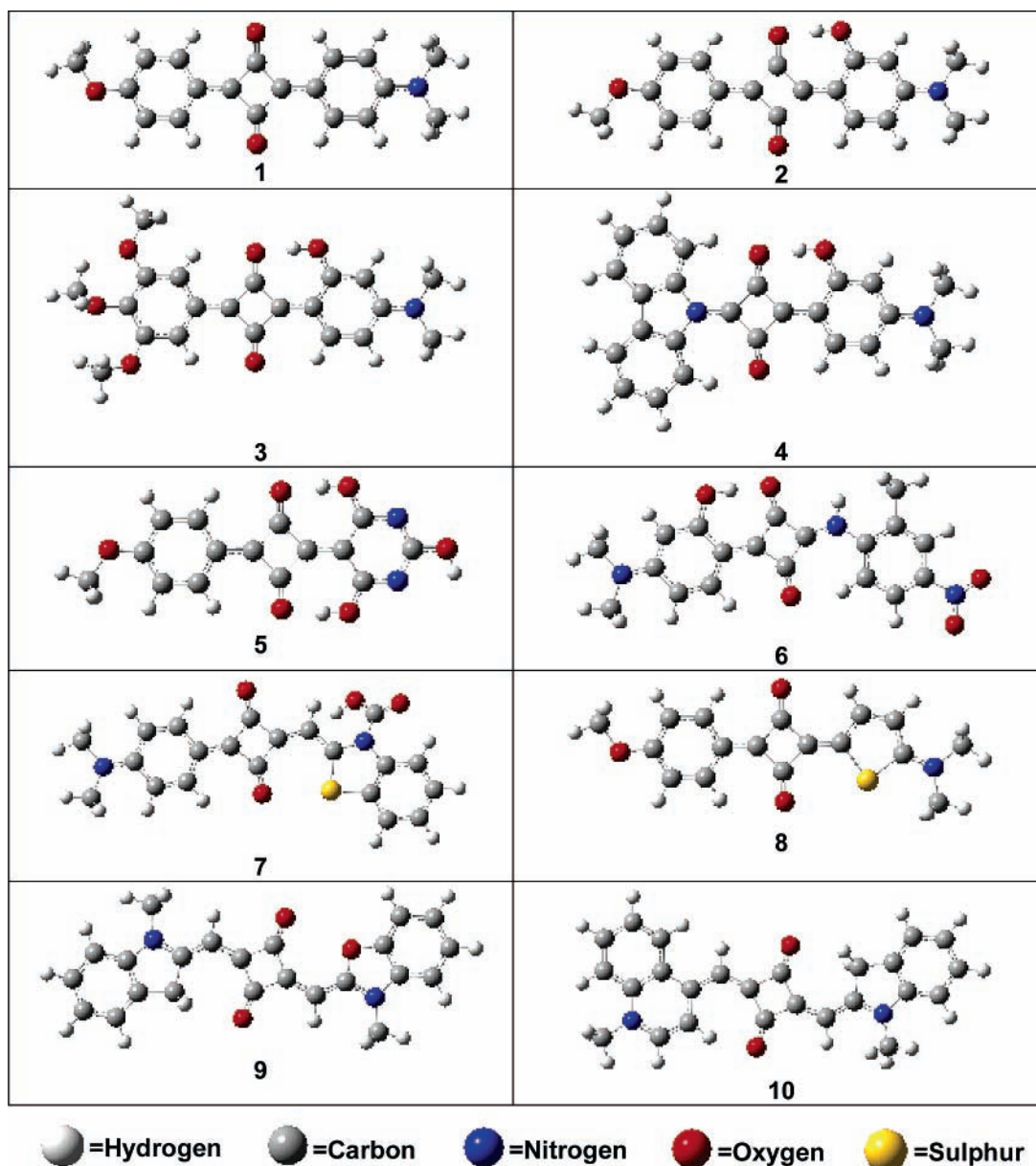
Unsymmetrical Squaraines

J. Phys. Chem. A, Vol. 110, No. 41, 2006 **11721**

Figure 1. Unsymmetrical squaraine molecules, **1**−**10**, which have been examined using SAC/SAC−CI in this study.

has lower occupation in the unsymmetrical case. The MOs of the HOMO and the LUMO are shown in Scheme 2. There is shift of the electron density to one side of the ring in the case of the unsymmetrical squaraine, as expected.

Using the above studies as a guideline, it is clear that there are fundamental differences in the structure and bonding which possibly would reflect in the nature of energy transitions in the symmetrical and unsymmetrical squaraines that would be best understood by carrying out high-level computational studies on the latter. This prompted us to carry out SAC−CI calculations on unsymmetric squaraines, with larger conjugation, to understand the role of the donor groups and the oxygen atoms. We study the charge transfer from the donor groups and the oxygen atoms and try to correlate the longer wavelength absorption and the nature of the donor groups. We also study the effect of solvent and also the effect of changing the basis sets on the transition energies.

Computational Details of the Higher Level Studies

For this study we have chosen 10 unsymmetrical SQ molecules with various donor groups and these are shown in Figure 1. In cases where the donor has a long alkyl chain, we have replaced it by the more symmetrical and computationally simpler CH_3 groups. This we found from our earlier studies, effects the transition energies to the maximum extent of 0.1 eV only.[2] Geometry optimization of all these molecules are carried out at B3LYP/6-31G(d,p) level inbuilt in the G03W software.[26] As we are interested in the ground state we target only the lowest singlet state for the optimization. Vibrational analysis (second order) is carried out to ensure that there are no negative frequencies and thus confirming that the stationary point obtained on the potential energy surface is indeed the minima. The ground-state singlet geometries obtained are then subjected to excited-state calculations to study the singlet−singlet transition.

For studying the nature of the excited-state transitions, we use SAC/SAC−CI.[29] SAC−CI methods have been applied for many molecules and found to be quite accurate for studying molecular spectroscopy.[30] Basically the SAC−CI is a cluster expansion method, and it is usually more rapidly convergent than CI. SAC−CI methods take into consideration the singly and doubly excited states, which mix up with the ground state

SCHEME 2. One Electron Molecular Orbital Pictures of Symmetrical and Unsymmetrical Squaraines Obtained at the B3LYP/6-31G(d,p) Level
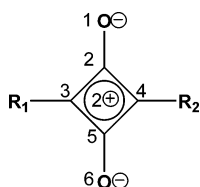

LUMO   LUMO

HOMO   HOMO

Symmetrical Squaraine   Unsymmetrical Squaraine
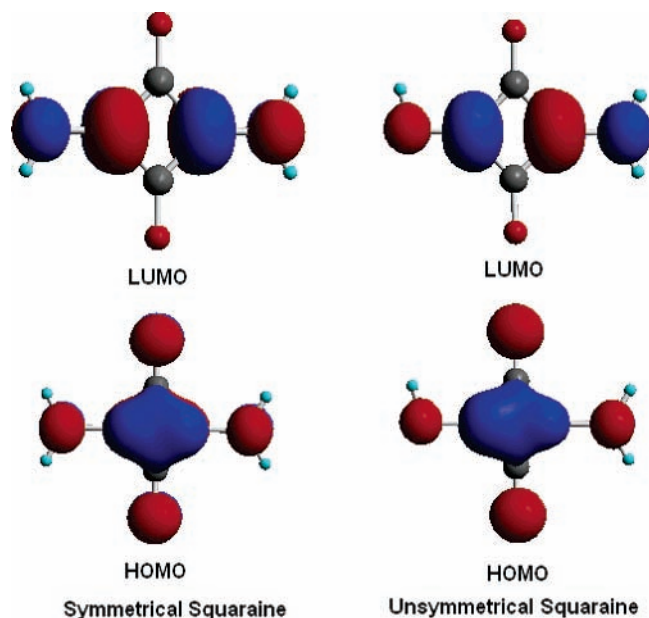
and the targeted excited state. More details of this method are available in the literature.[29] We had applied this technique in our previous study of dyes based on the oxyallyl substructure with success (a difference of less than 0.1 eV with the experimental observed excitation energy was obtained); hence, it is our choice for this study also.[2,6] In similar lines to our earlier study and earlier reports by other researchers, the optimized geometry of all the molecules obtained by DFT methods are subjected to SAC−CI.[30e]

For the ground state, SAC is carried out and is nonvariational, while for the excited state, SAC−CI is carried out using the variational methods. The active space is chosen with the window option where depending on the molecule's size some core and some virtual molecular orbitals are not used in the active space (but not less than 160 orbitals-all other details for each molecule are given in the tables). To the ground state, all the single excitation operators in this are also included without selection. For the doubles excitation operators an energy threshold value is used to select the configurations based on the perturbation method (vide infra). The SAC−CI is restricted to singles and doubles linked operators, while the higher order operators are treated through unlinked operators. All the single excitation operators in this are also included without selection. For the double excitation operators in both SAC and SAC−CI, estimated using the perturbation approach, there are three levels of selection. Those which contribute with a energy threshold (in Hartree) larger than 1.0×10^{-5} (SAC) and 1.0×10^{-6} (SAC−CI) is referred to as level one, those with 5.0×10^{-6} (SAC) and 5.0×10^{-7} (SAC−CI), as level two, and those with 1.0×10^{-6} (SAC) and 1.0×10^{-7} (SAC−CI), as level three. On the basis of our earlier work on SQ, we have chosen level two for the SAC−CI studies.[2] To be consistent with the SAC/SAC−CI ordering of the MOs where Hartree−Fock (HF) orbitals are the starting point, the molecular orbital one electron energies reported and used for discussion in this paper are based on HF/6-31G level.

To study the solvent effects, we have used the IEFPCM model.[31] Inclusion of the solvent effect is carried out in similar lines to the calculations reported recently by Hasegawa et al.; here the HF orbitals are obtained using the SCRF model and then the SAC/SAC−CI is carried out on these orbitals.[32] We have also estimated the basis set effect by carrying out calculations independently using the D95V basis set.[33] The choice of this basis is because of its performance in earlier SAC/SAC−CI studies.[34]

TABLE 3: Optimized Geometrical Parameters of All Molecules Obtained at the B3LYP/6−31g(d,p) Level

molecule (symmetry)	bond length (Å)				bond angles (deg)		
	O_1-C_2 (O_6-C_5)	C_2-C_3 (C_3-C_5)	C_2-C_4 (C_4-C_5)	C_3-R_1 C_4-R_2	$O_1-C_2-C_3$ $(O_6-C_5-C_3)$	$O_1-C_2-C_4$ $(O_6-C_5-C_4)$	$C_3-C_2-C_4$ $(C_3-C_5-C_4)$
1	1.229	1.473	1.479	1.418	135.9	135.3	88.8
(C_s)	(1.229)	(1.472)	(1.478)	(1.408)	(135.8)	(135.4)	(88.8)
2	1.249	1.450	1.466	1.423	136.8	132.5	90.7
(C_s)	(1.225)	(1.473)	(1.492)	(1.394)	(136.2)	(135.0)	(88.7)
3	1.250	1.448	1.466	1.426	136.8	132.4	90.7
(C_1)	(1.223)	(1.474)	(1.495)	(1.392)	(136.6)	(134.8)	(88.6)
4	1.278	1.470	1.450	1.354	138.0	131.7	90.3
(C_s)	(1.226)	(1.493)	(1.470)	(1.403)	(137.9)	(133.5)	(88.6)
5	1.241	1.459	1.472	1.420	137.2	132.5	90.2
(C_s)	(1.242)	(1.457)	(1.471)	(1.389)	(137.1)	(132.5)	(90.4)
6	1.245	1.455	1.451	1.400	135.2	134.7	90.1
(C_1)	(1.225)	(1.482)	(1.484)	(1.343)	(135.1)	(137.0)	(87.8)
7	1.226	1.474	1.480	1.409	136.0	135.0	89.0
(C_1)	(1.231)	(1.473)	(1.479)	(1.399)	(135.0)	(135.9)	(89.1)
8	1.228	1.469	1.486	1.422	136.6	134.6	88.7
(C_s)	(1.228)	(1.469)	(1.480)	(1.381)	(137.0)	(134.0)	(88.9)
9	1.225	1.479	1.484	1.401	134.0	137.2	88.8
(C_s)	(1.233)	(1.476)	(1.473)	(1.397)	(136.9)	(133.7)	(88.4)
10	1.231	1.479	1.477	1.392	133.7	136.6	89.7
(C_1)	(1.234)	(1.484)	(1.470)	(1.402)	(136.6)	(133.6)	(89.8)

Unsymmetrical Squaraines

J. Phys. Chem. A, Vol. 110, No. 41, 2006 **11723**

TABLE 4: Mixing Coefficients, Transition Dipole Moments (μ_{Ge} in Debye) for First Three Excited States Obtained from SAC−CI Method (level two/6-31G) at B3LYP/6-31G (d,p) Optimized Geometries

state	main configuration (|C| > 0.15)	ΔE (eV)	f	μ_{ge} X	μ_{ge} Y	μ_{ge} Z	expt ΔE (eV)[a]
		Molecule **1**					
1A′	0.94 (81A″−82A″)	2.15	1.28	1.04	−12.50	0.00	2.14
1A″	0.93 (76A′−82A″) + 0.16 (81A″−86A″; 75A′−82A″)	2.36	0.00	0.00	0.00	3 × 10⁻³	
2A″	0.93 (75A′−82A″) + 0.20 (81A″−86A″; 76A′−82A″)	3.67	2 × 10⁻³	0.00	0.00	−0.36	
		Molecule **2**					
1A′	0.93 (85A″−86A″)	2.10	1.18	1.35	12.10	0.00	2.20
1A″	0.93 (80A′−86A″)	2.74	1 × 10⁻⁴	0.00	0.00	0.08	
2A′	0.86 (84A″−86A″) − 0.30 (83A″−86A″) − 0.21(85A″−86A″, 84A″−86A″)	3.19	0.08	1.07	−2.31	0.00	
		Molecule **3**					
1A	0.93 (101A−102A)	2.26	1.25	12.07	0.16	0.16	2.21
2A	0.94 (96A−102A)	3.15	2 × 10⁻⁴	0.05	0.02	0.10	
3A	0.71 (99A−102A) − 0.57 (98A − 102A) −0.20 (101A−102A; 99A−102A)	3.30	0.09	−2.30	1.23	0.02	
		Molecule **4**					
1A′	0.93 (100A″−101A″)	2.35	1.27	−11.95	0.33	0.00	2.18
2A′	0.77 (97A″−101A″) − 0.49 (98A″−101A″) −0.17(100A″−101A″; 97A″−101A″)	3.59	0.07	1.91	1.20	0.00	
1A″	−0.93 (93A′−101A″) − 0.16 (100A″−103A″; 91A′−101A″)	3.67	1 × 10⁻⁴	0.00	0.00	0.09	
		Molecule **5**					
1A′	0.94 (81A″−82A″)	2.33	1.08	−1.05	−11.02	0.00	2.56
1A″	0.81 (77A′−82A″) − 0.48 (75A′−82A″)	2.97	0.00	0.00	0.00	5 × 10⁻⁴	
2A″	−0.79 (75A′−82A″) − 0.45 (77A′−82A″) −0.19 (77A′−84A″) − 0.17 (75A′−84A″)	3.90	0.00	0.00	0.00	−0.03	
		Molecule **6**					
1A	0.93 (96A−97A) − 0.15 (96A−98A)	2.46	1.35	11.99	−1.20	−1 × 10⁻³	2.25
2A	0.88 (95A−97A) + 0.24 (95A−98A) − 0.17 (94A−97A) 0.22 (96A−97A; 95A−97A)	3.63	0.05	1.36	−1.45	2 × 10⁻⁴	
3A	0.91 (91A−97A) + 0.24 (91A−98A) + 0.16 (96A−99A; 88A−97A)	3.76	5 × 10⁻⁴	7 × 10⁻⁴	2 × 10⁻³	−0.09	
		Molecule **7**					
1A	0.94 (102A−103A)	1.94	1.23	12.95	−0.07	0.02	1.99
2A	−0.93 (97A−103A) − 0.17 (102A−108A; 95A−103A)	2.59	2 × 10⁻³	−0.40	0.08	−0.06	
3A	0.60 (100A−103A) − 0.42 (101A−103A) 0.41 (99A−103A) − 0.19 (96A−103A) + 0.25 (102A−103A; 101A−103A) − 0.16 (102A−103A; 100A−103A)	3.65	0.15	−3.21	0.56	−0.07	
		Molecule **8**					
1A′	0.93 (82A″−83A″)	1.95	1.07	3.78	−11.43	0.00	2.20
1A″	0.93 (78A′−83A″) − 0.17 (82A″−86A″; 76A′−83A″)	2.31	0.00	0.00	0.00	−0.02	
2A″	0.92 (76A′−83A″) + 0.20 (82A″−86A″; 78A′−83A″)	3.64	1.6 × 10⁻³	0.00	0.00	−0.34	
		Molecule **9**					
1A′	0.94 (97A″−98A″)	2.04	1.25	4.05	−12.04	0.00	2.04
1A″	0.93 (93A′−98A″) + 0.19 (97A″−103A″; 90A′−98A″)	2.85	0.00	0.00	0.00	−0.04	
2A″	0.92 (90A′−98A″) + 0.26 (97A″−103A″; 93A′−98A″)	4.12	3 × 10⁻³	0.00	0.00	−0.44	
		Molecule **10**					
1A	−0.73 (100A−101A)	1.79	0.88	11.36	0.27	−0.02	1.82
2A	0.91 (96A−101A) + 0.16 (96A−102A) + 0.18 (100A−107A; 92A−101A)	3.05	3 × 10⁻³	−0.48	−0.06	−8 × 10⁻³	
3A	0.56 (100A−102A) + 0.46 (98A−101A) + 0.26 (99A−101A) − 0.16 (94A−101A) − 0.15 (100A−106A) + 0.34 (100A−101A; 100A−101A) + 0.17 (100A−101A; 99A−101A)	3.58	0.11	−2.68	0.74	0.01	

[a] Molecules **1−6** and **8−10** are in chloroform while molecule **7** is in benzene.

Results and Discussion

(a) Geometry. To the best of our knowledge there are no reported experimental (crystal data) bond lengths and bond angles of unsymmetrical SQ. A search in the CSD database reveals that there are only about 10 symmetrical SQ for which the crystal data is available.[35] Hence the geometrical parameters obtained in this section for the unsymmetrical SQ would be of immense help in understanding the nature of these molecules. The changes observed in the central ring with substitution would also reveal the nature of polarization and transition in these dyes. Furthermore, in this section, we shall compare the computationally obtained bond lengths and bond angles of the unsym-metrical SQ with that of the experimental data of the symmetrical SQ obtained from the CSD.

For the convenience of representing the unsymmetrical nature of the molecules the two donor groups are denoted as left and right side substituents i.e., at 3- and 4-positions in the figure. The two oxygen atoms in 2- and 5-positions are also not equal due to this asymmetry. The symmetry of the molecules is low as expected and is C_s (molecular plane) in most of the molecules except in four cases, **3**, **6**, **7**, and **10**. As we are interested in geometry changes due to unsymmetrical substitution at the central moiety, we report only those geometric parameters that are related to the C_4O_2 ring for all the molecules in Table 3.

TABLE 5: Dimensions of the Linked Operator and Configurations in the SAC/SAC−CI Calculations

		SAC			SAC−CI			
molecule	state[a]	before[c]	after[d]	no. of configurations[e]	state[a]	before[c]	after[d]	no. of configurations[e]
1	A′	6162470	36038	19	A′	6162470	122373	25
					A″	5948110	117220	
2[b]	A′	6126480	32800	10	A′	6126480	151060	23
					A″	5984100	186250	
3	A	12110580	21352	24	A	12110580	119707	31
4	A′	6078276	28846	29	A′	6078276	108159	24
					A″	6032304	96692	
5	A′	6171102	45253	9	A′	6171102	131280	22
					A″	5939478	144370	
6[b]	A	12110580	32584	25	A	12110580	147266	23
7	A	12110580	27885	29	A	12110580	131418	15
8[b]	A′	6162470	38727	12	A′	6162470	141484	22
					A″	5948110	171476	
9	A′	6080390	27738	35	A′	6080390	106588	21
					A″	6030190	115180	
10	A	12110580	24427	28	A	12110580	109973	24

[a] Number of solutions for SAC is one; for SAC−CI it is six. [b] Number of solutions for SAC−CI = 8. [c] Number of linked operatorss before selection. [d] Number of linked operators after selection. [e] Number of configurations that have a CI coefficient larger than 0.03.

From the geometric parameters it is observed that unsymmetrical substitution introduces deviations to the symmetrical ones. The stronger donor substituent forms stronger bonding with C_4O_2 ring and induces a quinoidal character in the phenylene ring while the weaker donor forms a weak bond and thus induces less quinoidal (more aromatic) character. The consequence of which, the carbon−oxygen (CO) and carbon−carbon (CC) bond lengths and carbon−carbon−carbon (CCC) and carbon−carbon−oxygen (CCO) bond angles in the central ring vary accordingly.

We could now approximately subdivide the molecules based on the obtained C−O bond length data into three groups. In the first case, the C−O bond lengths are around 1.229 Å and both the C−O bonds are almost equal. In the second group, we classify those molecules which again have nearly equal C−O bond lengths but now the bond lengths are much longer and are around 1.241−1.250 Å. In the third category, we have those molecules whose C−O bond lengths are unequal. In the case of symmetrical squaraines obtained form the CSD database we observe similar bond lengths as expected due to symmetry. The bond lengths obtained in the CSD database are around 1.226 Å and in some cases around 1.253 Å. A careful examination of both these symmetrical and unsymmetrical structures reveal that the long bond lengths are obtained in the cases where there is a hydrogen bonding of the side OH/NH group with the C−O bond, as shown in Figure 1. In other words, the hydrogen bond stabilizes the negative charge on the oxygen atom and hence the bond order of these bonds decrease. As these molecules are known to exhibit charge-transfer transitions this observation that the hydrogen bond stabilizes the O$^-$ atom retaining a larger negative charge, and a lower bond order is of great importance.

Individual examination of the geometry is now carried out. The C−O bond in molecule **1** and **8** is around 1.228−1.229 Å and the other C−O bond length is also the same. The bond angle of the C3−C2−C4 bond is around 88.8° and is almost equal to that of the C3−C5−C4 angle. However, the C−C bond lengths of the ring are unequal. The C−R bond lengths also have almost a difference of 0.010 Å. In molecules **2**, **3**, **4**, and **6** due to the one side H-bonding the bond lengths are unequal. And this is reflected in the bond angles also. In **2** the C−O bond length on the H-bonded side is around 1.249 Å while the one without the H-bond is shorter and is 1.225 Å. In the case of **3**, **4**, and **6**, a strong similarity with **2** is observed. In the

case of **5** the C−O bond lengths are longer (around 1.241 Å) and equal due to H-bonding on both sides. Another observation is that in molecules **7**, **9**, and **10** the inequalities of the donors result in a slight variation in the CO bond lengths i.e., 0.003−0.008 Å. This inequality also brings difference in CC bonds more pronounced in molecules **9** and **10** with a variation of 0.001−0.009 Å. The angle range obtained for the bond angles is 88−90°, which is in good agreement with the symmetric squaraines angles. The other consequence of the H-bonding is that the C−C bond adjacent to the H-bonded C−O has a smaller bond length or in other words a larger double bond character. Thus, we observe that the polarization due to the asymmetric substitution is not only on the long axis of the molecule but also on the short axis.

(b) SAC/SAC−CI Study. Absorption energies obtained by SAC−CI method are tabulated in Table 4. SAC improves the symmetric HF ground state of all the molecules, and the corresponding configurations contributing to this state are shown in Table 5. To the ground state in SAC the HF contribution will be 1.00 (as per definition), hence not shown. To understand the charge flow concept we shall concentrate on the crucial excited state configuration contributing to the ground state of all the molecules. The basic ground state configuration consists mainly with the association of double excitation, which comprises of frontier highest occupied and lowest unoccupied orbitals. Here in all molecules the mixing coefficient of HOMO−LUMO double excitation is around 0.04−0.06 in addition to some configurations from other lower and higher orbitals (not shown in the tables for clarity). The general inference is that by including this orbital excitation in the CI, the fully distributed charge on C_4O_2 ring in HOMO becomes disturbed, and it decreases the charge density at the center of ring and enhances the diradicaloid nature in to the ground state. In addition, the other main configurations, which have coefficient values of about 0.04−0.09, are involved in the charge delocalization through out the molecule. The major contributors to the excited state obtained at SAC−CI level (mixing coefficients of ≥0.15) are also given in the table. In contrast to the ground state, in the excited state the single excited state is the major contributor. In all the molecules the main contribution is from the HOMO−LUMO single excitation, which has larger coefficient values about 0.94 in most of the cases. There are
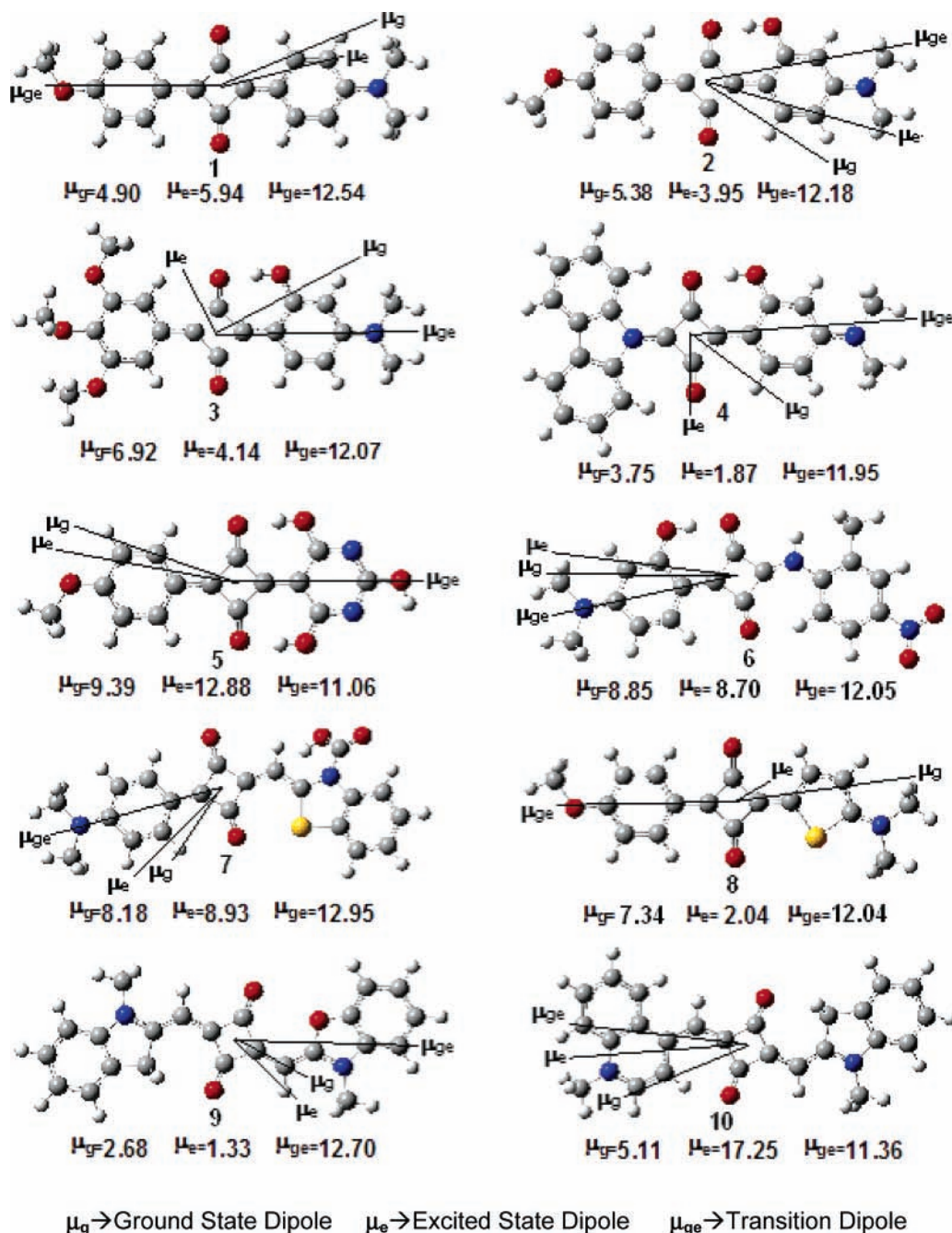
Unsymmetrical Squaraines

J. Phys. Chem. A, Vol. 110, No. 41, 2006 **11725**

$\mu_g \rightarrow$ Ground State Dipole $\mu_e \rightarrow$ Excited State Dipole $\mu_{ge} \rightarrow$ Transition Dipole

Figure 2. Dipole direction in ground and excited states along with the transition dipole vectors for all the molecules obtained using SAC/SAC−CI methods at B3LYP/6-31G (d,p) optimized geometries.

some small contributions from other excitations that gives rise to the charge distribution through out the molecule. Only in the case of **10** does the coefficient drop down to 0.73, and the other coefficients, being less than 0.15, are not indicated in the table.

From Table 4 it is clear that the absorption energy data obtained by SAC−CI method is in good agreement with the experimental data. The deviation, in absolute values, is maximum of 0.25 eV obtained in the case of molecule **8** and 0.23 eV in the case of molecule **5**. But the trend is well reproduced. Comparing **1**, **2**, **3**, and **4** shows that the experimental determined absorption energy varies to the maximum of only 0.01 eV from 2.15 eV in **1**. The ΔE for **2** obtained by calculations deviates from the experimental value by 0.12 eV. In the case of **3** we see that the deviation is only 0.05 eV. 0.17 eV is the deviation in the case of **4**. A slight overestimation is seen in the case of

4. In the case of **5** and **6** the deviation with the experimental value is slightly larger and is greater than 0.2 eV. Replacing the donor group in **1** by a heterocyclic ring in **5** blue shifts the absorption by 0.4 eV, and this is predicted by SAC−CI to be around 0.18 eV. In the case of **10**, there is a red shift of around 0.3 eV compared to **1**, which is well predicted by SAC−CI methods to be around 0.3 eV. We have also calculated the next two lower transitions and tabulated them in the same table. In most of the cases these transitions are forbidden. The next lowest transition is almost of the same magnitude as the lowest energy transition, while the next higher one is slightly larger by 2 eV in most of the cases.

The excited-state dipole moment along with the ground-state dipole moment and their components are shown in Figure 2. In most of the cases the ground-state dipole moment and the excited-state dipole moment are in the same direction. In **1**, **5**,
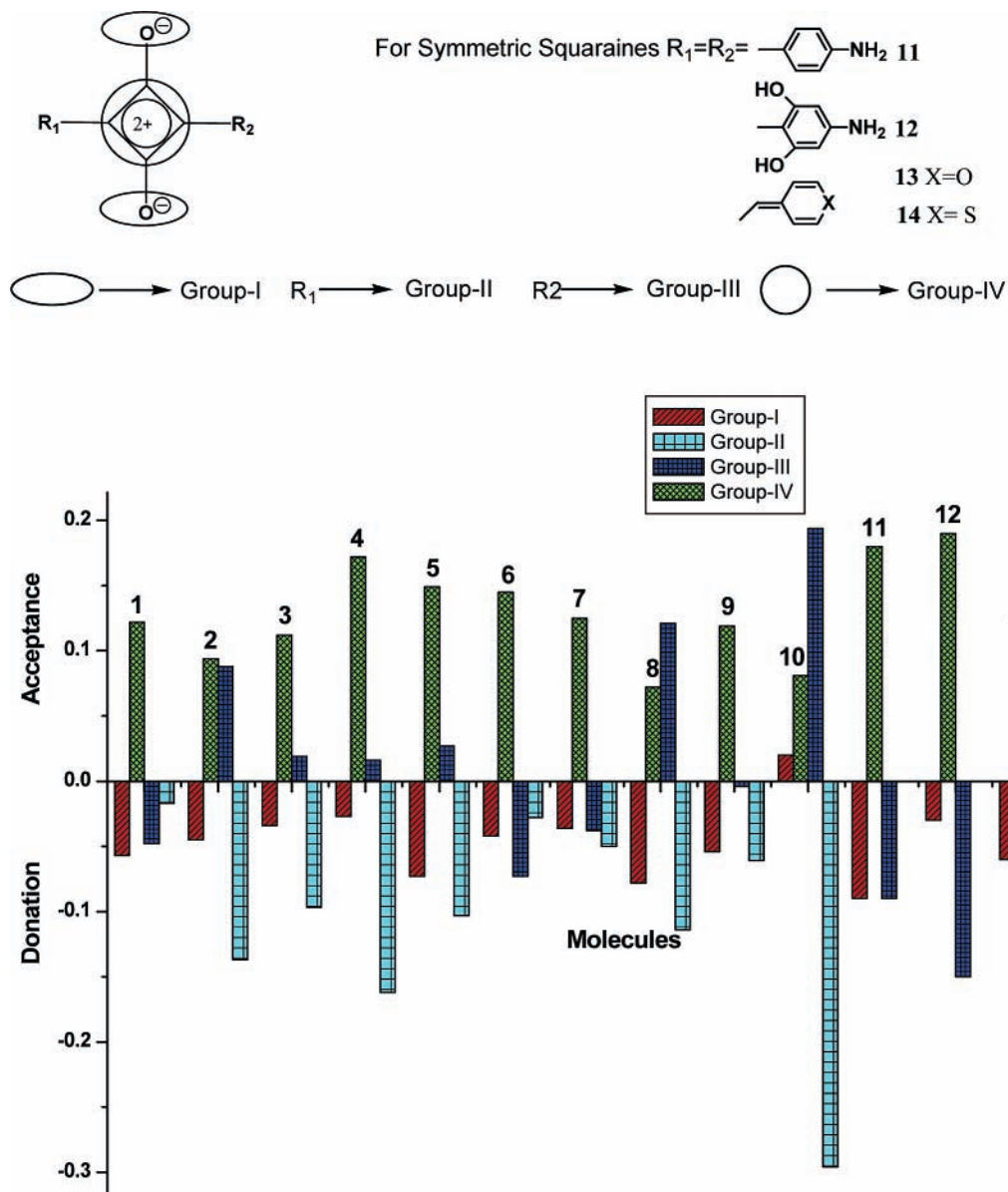
Figure 3. Comparison of charge donation and acceptance of groups I–IV for unsymmetrical (**1**–**10**) and symmetrical (**11**–**14**) squaraines. Charge-transfer data for symmetric molecules are taken from ref 2.

6, and **7** the dipole moments lie in the same direction, while in the others there is a small deviation. The ground-state dipole moment of **1**, **7**, and **9** hardly changes in the excited state (maximum of 1.5 D). While in **2**, **3**, and **4** there is a change in the absolute magnitude of around 2.0 D upon excitation, in **1**, **5**, **6**, **7**, and **10** the dipole moment increases upon excitation. Only in the case of **10** is the increase very high, 12 D. There is a varied behavior in change in dipole moments depending on the donor groups which thus cannot be generalized. This is in contrast to the symmetrical SQ, where due to symmetry there is no dipole moment in the ground state.[2]

The transition dipole moment shown in the same figure indicates a large moment in the direction of the long axis. The intensity arises from the π-conjugation of the backbone as in a typical $\pi-\pi^*$ transition. The values are quite large and almost in the same range of 11.0–13.0 D for all molecules. The corresponding oscillator strengths are also very high and are around 0.88–1.40 (shown in Table 4). In the case of **2**, **3**, **7**, and **10** there is some significant oscillator strength for the higher energy transitions also.

The calculated absorption energy in the presence of a solvent is shown in Table 6. The solvent model IEFPCM is used only for generating the HF orbitals on which the SAC/SAC–CI is carried out. We find a slightly better agreement with the experimental values in the case of molecules **2**, **5**, and **8**. In **7** and **10**, the absorption bands are not shifted at all while there is a very small shift in the case of molecules **4**, **6**, and **9**. Overall, including the solvent effects (like chloroform) makes only a small difference to the absorption energy values.[37] The effect of changing the basis set on the absorption energies is also shown in the same table. We have carried out the calculation for both gas phase and solvent phase using the D95V basis. Here due to lack of parameters we were unable to calculate the absorption energies of **7** and **8**. The change of basis has nearly no major effect on the magnitude of the absorption energies (the maximum shift is in the case of molecule **10**, which is only 0.17 eV).

(c) Charge transfer. To get a clear understanding of the charge delocalization in the ground and excited states of unsymmetrical SQ dyes, we have tabulated the total charge

Unsymmetrical Squaraines

J. Phys. Chem. A, Vol. 110, No. 41, 2006 **11727**

TABLE 6: Basis Set and Solvent Effects on the Excited States of Molecules 1−10 Calculated by the SAC−CI Method

| molecule | 6-31G(D95V) | | | | exptl ΔE (eV)[b] |
| | gas phase | | IEFPCM Model with solvent | | |
	ΔE (eV)	f	ΔE (eV)	f	
1	2.15	1.28	2.18	1.44	2.14[c]
	(2.11)	(1.26)	(2.18)	(1.45)	
2	2.10	1.18	2.15	1.28	2.2[c]
	(2.03)	(1.13)	(2.12)	(1.20)	
3	2.26	1.25	2.35	1.38	2.21[c]
	(2.17)	(1.21)	(2.26)	(1.34)	
4	2.35	1.27	2.36	1.36	2.18[d]
	(2.29)	(1.29)	(2.32)	(1.38)	
5	2.33	1.08	2.34	1.11	2.56[e]
	(2.22)	(1.04)	(2.23)	(1.06)	
6	2.46	1.35	2.48	1.46	2.25[d]
	(2.47)	(1.40)	(2.43)	(1.34)	
7[a]	1.94	1.23	1.94[b]	1.30	1.99[f]
8[a]	1.95	1.07	2.04	1.20	2.2[g]
9	2.04	1.25	2.05	1.33	2.04[h]
	(2.00)	(1.25)	(2.03)	(1.38)	
10	1.79	0.88	1.79	0.85	1.82[i]
	(1.62)	(1.20)	(1.64)	(1.24)	

[a] Molecules **7** and **8** include sulfur for which **D95V** basis set is not defined. [b] Molecules **1−6** and **8−10** are in chloroform while molecule **7** is in benzene. [c] Reference 9. [d] Reference 22. [e] Reference 21. [f] Reference 17a. [g] Reference 18a. [h] Reference 19a. [i] Reference 20a.

Figure 4. Variation of HOMO−LUMO gap (eV) with respect to excitation energy (eV) for molecules **1−10**.

Figure 5. Variation of charge transfer (central ring acceptance) with respect to excitation energy (eV) for molecules 1−10.

density and charge-transfer data in Figure 3. These values are Mulliken charges obtained at SAC and SAC−CI levels for ground and excited states, respectively. For the sake of convenience in understanding the charge transfer, the molecule is divided into four parts. Two oxygen atoms from two carbonyl groups are assumed as group I, left and right side substituents are group II and group III, respectively, and finally the central C_4 ring is group IV. The charge transfer is now discussed based on this division. In molecule **1**, the charge on oxygen atoms is of −1.142 in ground state and after excitation reduces to −1.085 with the loss of −0.057 charge. The charges on group II and III in ground and excited states are 0.378, 0.426 and 0.270, 0.287, respectively, with a small loss of −0.048 and −0.017e on excitation. The charge gain in group IV is 0.122 from ground to excited state. Thus, both the side donor groups and the oxygen atoms (major donor) act as a donor while the carbon ring acts as an acceptor. This is in agreement with the results obtained by Bigelow and Freund for symmetric SQ.[10] They found that the oxygen atoms donate up to −0.180e to the central moiety. In another report by Bredas and co-workers on the NLO properties of unsymmetrical SQ, it was found that there was very little charge transfer to the central ring form the donor groups.[36] These studies are in good agreement with our work here. In molecule **2**, due to hydrogen bonding from group III to the oxygen atom, the charge transfer from the oxygen atoms is reduced to −0.045 compared to the previous molecule. And also this effect leads to a charge-transfer i.e. −0.137 from group III and gain of 0.088 in the other group II. The central acceptor gains around 0.094 charge on excitation, less than what was observed for molecule **1**. A similar kind of behavior is observed in molecule **3**; the difference in donor abilities of group II and III are reflected as a −0.097 charge loss in one donor group while the other donor group has a net charge gain of 0.019. Here the charge transfer from the oxygen atoms drop down to −0.034. The situation in molecules **5** and **8** is also not so different. Here charge donation from group I and acceptance in IV are of −0.073 and +0.149, −0.099 and +0.069 charge,
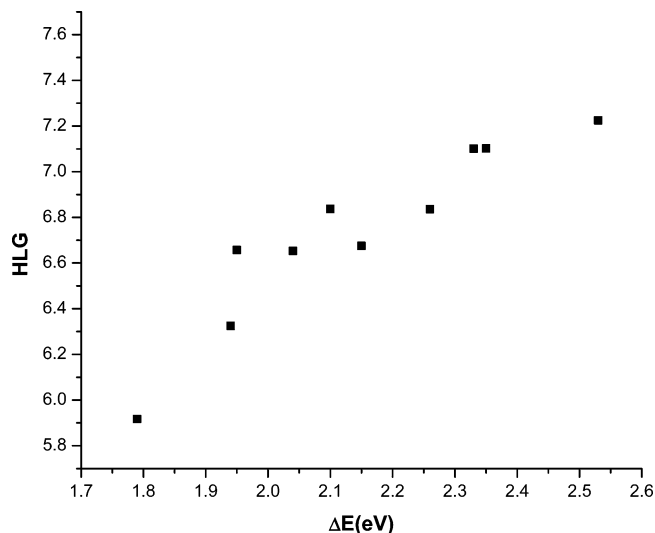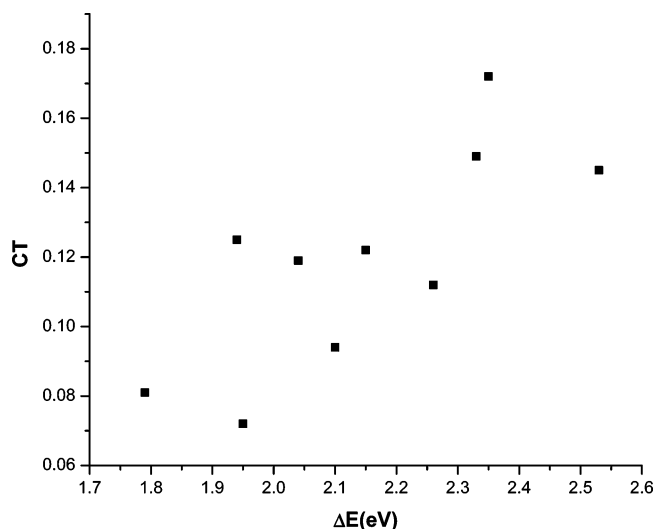
respectively. Since stabilization of the charge on the oxygen atom due to hydrogen bonding takes place in molecule **4**, the donation from group I is reduced to −0.027. In molecule **4**, the donation and gain of charges in group II and III are of same order, −0.162 and +0.016, respectively, and evidently, a large charge transfer to group IV is observed, 0.172. However, in molecules **6** and **7**, the charge moves from both right side substituent and the left side one to the central ring. The remaining two molecules **9** and **10** are of different natures with respect to each other in the context of charge transfer. In molecule **9**, charge donation from group I is −0.054 and to group IV a large value of 0.119. And also the loss of charge in group III is of −0.061 whereas for the group II a very small amount of charge gain is observed, i.e., −0.004e. On the other hand in molecule **10** unlike in **9**, a small charge gain in group I is seen i.e., 0.020. On the other hand the prominent charge transfer from the group II and group III is observed: +0.194 and −0.296 of gain and loss of group II and group III, respectively. Also a gain of 0.087 in group IV is observed.

For comparison, we have included the CT values of symmetrical SQ obtained from an earlier study.[2] We see that the donor groups always donate along with oxygen to the central ring, in marked contrast to the unsymmetrical case.

To understand whether the red-shift arises due to larger charge transfer from the donor groups in these molecules, we have correlated the HLG with the absorption energy in Figure 4, and in Figure 5 we have the variation of the charge acceptance of the central ring vs the absorption energy. It is seen that the absorption energy increases with the increase in HLG. This is in fact in line with our earlier studies on symmetric squaraines.[2,6] On the other hand the charge donation does not have any correlation with the ΔE. The larger charge transfer occurring in one or two molecules are seen in the higher energy side. This clearly shows that in the excited state the donating capacity of the side donor groups does not play a role in the red shift of the absorption.

Conclusions

NBO and NRT studies indicate that there are some differences in resonance structure and weights, bond orders and valencies in symmetrical and unsymmetrical squaraines. There is also a larger ionic character for one of the oxygen atoms of the squaraine ring in the unsymmetrical case. SAC/SAC−CI studies are in good agreement with the experimental data. With the inclusion of solvent effects a slightly better agreement with experimental value is seen in some cases. Basis set changes do not effect the magnitude of the predicted absorption energies. Earlier studies on symmetrical SQ using SAC/SAC−CI methods indicate that the lowest energy transitions take place with small charge transfer from the donor rings and oxygen atoms into the central ring. However, in the case of unsymmetrical squaraines, it is found here that the charge transfer could be from either donor ring or both rings into the central ring and in some cases can be from one donor ring to the other. The oxygen atoms mostly act as donors but in some few cases also as acceptors. Both from the earlier SAC/SAC−CI study on symmetrical squaraines and this study on unsymmetrical squaraines, it is found that the amount of charge transfer in the excited state has no correlation with the lowest energy transition, and hence, these could be classified as charge rearrangement kind of transitions occurring in diradicaloids and not charge-transfer transitions. The donor groups stabilize the resonance structures in the ground state. A correlation of the energy transition is seen with the HOMO−LUMO gap (indicative of the diradical nature of the diradicaloid system). The lowering of HOMO−LUMO gap always leads to a bathochromic shift. We conclude that there is no distinctive advantage in absorption characteristics in unsymmetrical squaraines over that of the symmetrical squaraines except that these squaraines have dipole moment in the ground state.

References and Notes

(1) Fabian, J.; Zahradnik, R. *Angew. Chem., Int. Ed.* **1989**, *28*, 677.

(2) Prabhakar, Ch.; Yesudas, K,; Krishna Chaitanya, G.; Sitha, S.; Bhanuprakash, K.; Jayathritha Rao, V. *J. Phys. Chem. A* **2005**, *109*, 8604.

(3) Neuse, E. W.; Green, B. R. *J. Am. Chem. Soc.* **1975**, *97*, 3987.

(4) Simard, T. P.; Yu, J. H.; Zebrowski-Young, J. M.; Haley, N. F.; Detty, M. R. *J. Org. Chem.* **2000**, *65*, 2236.

(5) Wirz, J. *Pure Appl. Chem.* **1984**, *56*, 1289.

(6) Prabhakar, Ch.; Krishna Chaitanya, G.; Sitha, S.; Bhanuprakash, K.; Jayathritha Rao, V. *J. Phys. Chem. A* **2005**, *109*, 2614.

(7) Fabian, J. *Chem. Rev.* **1992**, *92*, 1197.

(8) Law, K. Y. *Chem. Rev.* **1993**, *93*, 449.

(9) Law, K. Y. *J. Org. Chem.* **1992**, *57*, 3278.

(10) Bigelow, R. W.; Freund, H. J. *Chem. Phys.* **1986**, *107*, 159.

(11) (a) Meier, H.; Petermann, R. *Helv. Chim. Acta* **2004**, *87*, 1109. (b) Langhals, H. *Angew. Chem., Int. Ed.* **2003**, *42*, 4286. (c) Meier, H.; Dullweber, U. *J. Org. Chem.* **1997**, *62*, 4821. (d) Meier, H.; Dullweber, U. *Tetrahedron Lett.* **1996**, *37*, 1191. (e) Law, K. Y. *J. Phys. Chem.* **1987**, *91*, 5184.

(12) (a) Tian, M.; Tatsuura, S.; Furuki, M.; Sato, Y.; Iwasa, I.; Pu, L. S. *J. Am. Chem. Soc.* **2003**, *125*, 348. (b) Tatsuura, S.; Tian, M.; Furuki, M.; Sato, Y.; Iwasa, I.; Mitsu, H. *Appl. Phys. Lett.* **2004**, *84*, 1450. (c) Tatsuura, S.; Mastubara, T.; Tian, M.; Mitsu, H.; Iwasa, I.; Sato, Y.; Furuki, M. *Appl. Phys. Lett.* **2004**, *85*, 540. (d) Detty, M. R,; Henne, B. *Heterocycles.* **1993**, *35*, 1149. (e) Law, K. Y,; Bailey, F. C. *Dyes Pigm.* **1993**, *21*, 1.

(13) Meier, H.; Petermann, R.; Gerold, J. *Chem. Commun.* **1999**, 977. (b) Bello, K. A,; Ajayi, J. O. *Dyes Pigm.* **1996**, *31*, 79. (c) Park, S.-Y,; Jun, K,; Oh, S.-W. *Bull. Korean Chem. Soc.* **2005**, *26*, 428. (d) Law, K. Y,; Bailey, F. C. *Dyes Pigm.* **1988**, *9*, 85. (e) Matsui, M,; Tanaka, S,; Funabiki, K,; Kitaguchi, T. *Bull. Chem. Soc. Jpn.* **2006**, *79*, 170.

(14) (a) Jyothish, K.; Arun, K. T.; Ramaiah, D. *Org. Lett.* **2004**, *6*, 3965. (b) Ramaiah, D,; Eckert, I,; Arun, K. T,; Weidenfeller, L,; Epe, B. *Photochem. Photobiol.* **2004**, *79*, 99. (c) Keil, D. *Dyes Pigm.* **1991**, *17*, 19. (d) Kuramoto, N,; Natsukawa, K,; Asao, K. *Dyes Pigm.* **1989**, *11*, 21. (e) Kukrer, B,; Akkaya, E. U. *Tetrahedron Lett.* **1999**, *40*, 9125.

(15) (a) Beverina, L.; Abbotto, A.; Landenna, M.; Cerminara, M.; Tubino, R.; Meinardi, F.; Bradamante, S.; Pagani, G. A. *Org. Lett.* **2005**, *7*, 4257. (b) Chenthamarakshan, C. R,; Ajayaghosh, A. *Chem. Mater.* **1998**, *10*, 1657. (c) Kim, S.-H.; Hwang, S. H. *Dyes Pigm.* **1997**, *35*, 111. (d) Santos, P,; Reis, L. V.; Duarte, I,; Serrano, J. P.; Almeida, P,; Oliveira, A. S,; Ferreira, L. F. V. *Helv. Chim. Acta* **2005**, *88*, 1135. (e) Ramaiah, D,; Arun, K. T. *J. Phys. Chem. A* **2005**, *109*, 5571.

(16) Ajayaghosh, A. *Acc. Chem. Res.* **2005**, *38*, 449.

(17) (a) Alex, S,; Santhosh, U,; Das, S. *J. Photochem. Photobiol. A: Chem.* **2005**, *72*, 63. (b) Kim, J. J.; Funabiki, K.; Shiozaki, H.; Matsui, M. *Dyes Pigm.* **2003**, *57*, 165. (c) Law, K. Y. *Chem. Mater.* **1992**, *4*, 605.

(18) (a) Keil, D.; Hartmann, H. *Dyes Pigm.* **2001**, *49*, 161. (b) Law, K. Y. *J. Phys. Chem.* **1995**, *99*, 9818. (c) Yagi, S,; Hyodo, Y,; Matsumoto, S,; Takahashi, N,; Kono, H,; Nakazumi, H. *J. Chem. Soc., Perkin Trans. 1* **2000**, 599. (d) Chen, J.-G,; Huang, D.-Y,; Li, Y. *Dyes Pigm.* **2000**, *46*, 93.

(19) (a) Tatarets, A. L,; Fedyunyaeva, I. A,; Terpetschnig, E,; Patsenker, L. D. *Dyes Pigm.* **2005**, *64*, 125. (b) Law, K. Y. *Chem. Phys. Lett.* **1992**, *200*, 121. (c) Law, K. Y,; Bailey, C. *J. Chem. Soc., Chem. Commun.* **1990**, 863. (d) Terpetschnig, E,; Lakowicz, J. R. *Dyes Pigm.* **1993**, *21*, 227.

(20) (a) Kim, S.-H.; Hwang, S.-H.; Kim, N.-K.; Kim, J.-W.; Yoon, C.-M.; Keum, S.-R. *J. S. D. C.* **2000**, *116*, 127. (b) Chen, C.-T,; Marder, S. R,; Cheng, L.-T. *J. Am. Chem. Soc.* **1994**, *116*, 3117.

(21) Marder, S.; Chen, C−T. U.S. Patent. 5,500,156, 1996.

(22) Shimizu, Toyoda, Kinugasa, Yamada, Ikuta, Mutoh, Satoh, and Tomura et al. Eur. Patent 1,152,037 A9, 2001.

(23) Momicchioli, F.; Tatikolov, A. S.; Vanossi, D.; Ponterini, G. *Photochem. Photobiol. Sci.* **2004**, *3*, 396.

(24) NBO 5.0. Glendening, E. D.; Badenhoop, J. K.; Reed, A. E.; Carpenter, J. E.; Bohmann, J. A.; Morales, C. M.; Weinhold, F. Theoretical Chemistry Institute, University of Wisconsin: Madison, WI, 2001; http://www.chem.wisc.edu/~nbo5.

(25) (a) Glendening, E. D.; Weinhold, F. *J. Comput. Chem.* **1998**, *19*, 593. (b) Glendening, E. D.; Weinhold, F. *J. Comput. Chem.* **1998**, *19*, 610. (c) Glendening, E. D.; Badenhoop, J. K.; Weinhold, F. *J. Comput. Chem.* **1998**, *19*, 628.

(26) Frisch, M. J.; Trucks, G. W.; Schlegel, H. B.; Scuseria, G. E.; Robb, M. A.; Cheeseman, J. R.; Montgomery, J. A., Jr.; Vreven, T.; Kudin, K. N.; Burant, J. C.; Millam, J. M.; Iyengar, S. S.; Tomasi, J.; Barone, V.; Mennucci, B.; Cossi, M.; Scalmani, G.; Rega, N.; Petersson, G. A.; Nakatsuji, H.; Hada, M.; Ehara, M.; Toyota, K.; Fukuda, R.; Hasegawa, J.; Ishida, M.; Nakajima, T.; Honda, Y.; Kitao, O.; Nakai, H.; Klene, M.; Li, X.; Knox, J. E.; Hratchian, H. P.; Cross, J. B.; Adamo, C.; Jaramillo, J.; Gomperts, R.; Stratmann, R. E.; Yazyev, O.; Austin, A. J.; Cammi, R.; Pomelli, C.; Ochterski, J. W.; Ayala, P. Y.; Morokuma, K.; Voth, G. A.; Salvador, P.; Dannenberg, J. J.; Zakrzewski, V. G.; Dapprich, S.; Daniels, A. D.; Strain, M. C.; Farkas, O.; Malick, D. K.; Rabuck, A. D.; Raghavachari, K.; Foresman, J. B.; Ortiz, J. V.; Cui, Q.; Baboul, A. G.; Clifford, S.; Cioslowski, J.; Stefanov, B. B.; Liu, G.; Liashenko, A.; Piskorz, P.; Komaromi, I.; Martin, R. L.; Fox, D. J.; Keith, T.; Al-Laham, M. A.; Peng, C. Y.; Nanayakkara, A.; Challacombe, M.; Gill, P. M. W.; Johnson, B.; Chen, W.; Wong, M. W.; Gonzalez, C.; Pople, J. A. *Gaussian 03*, revision B.01. Gaussian, Inc.: Wallingford CT, 2004.

(27) Feldgus, S.; Landis, C. R.; Glendening, E. D.; Weinhold, F. *J. Comput. Chem.* **2000**, *21*, 411.

(28) A fully functional stand-alone NBO5.0 implementation, which can be used to execute FILE47, obtained from any standard ab initio program.

(29) Nakajima, T.; Nakatsuji, H. *Chem. Phys. Lett.* **1999**, *300*, 1.

(30) (a) Wan, J.; Ehara, M.; Hada, M.; Nakatsuji, H. *J. Chem. Phys.* **2000**, *113*, 5245. (b) Wan, J.; Hada, M.; Ehara, M.; Nakatsuji. M. *J. Chem. Phys.* **2001**, *114*, 842. (c) Nakatsuji, H. *Acta Chim. Hung.* **1992**, *129*, 719. (d) Nakatsuji, H. In *Computational Chemistry—Reviews of Current Trends*; Leszczynski, J., Ed.; World Scientific: River Edge, NJ, 1997; Vol. 2. (e) Hu, Z.; Boyd, R. J.; Nakatsuji, H. *J. Am. Chem. Soc.* **2002**, *124*, 2664.

(31) (a) Cances, M. T.; Mennucci, B.; Tomasi, J. *J. Chem. Phys.* **1997**, *107*, 3032. (b) Mennucci, B.; Tomasi, J. *J. Chem. Phys.* **1997**, *106*, 5151. (c) Mennucci, B.; Cances, E.; Tomasi, J. *J. Phys. Chem. B* **1997**, *101*, 10506. (d) Tomasi, J.; Mennucci, B.; Cances, E. *J. Mol. Struct. (THEOCHEM)* **1999**, *464*, 211.

(32) Hasegawa, J.-Y.; Takata, K.; Miyahara, T.; Neya, S.; Frisch, M. J.; Nakatsuji, H. *J. Phys. Chem. A* **2005**, *109*, 3187.

(33) Dunning, T. H., Jr.; Hay, P. J. *Modern Theoretical Chemistry*; Plenum: New York, 1976; Vol. 3, p 1.

(34) Honda, Y.; Hada, M.; Ehara, M.; Nakatsuji, H. *J. Phys. Chem. A* **2002**; *106*, 3838.

(35) Cambridge Crystallographic Data Center (CCSD). 12 Union Road, Cambridge CB2 1EZ, England.

(36) Meyers, F.; Chen, C. T.; Marder, S. R.; Bredas, J.-L. *Chem.—Eur. J.* **1997**, *3*, 530.

(37) Carrying out calculations using highly polar solvent like DMSO we find a blue shift in the case of molecule **3** and a red shift in the case of molecule **10.** This is in agreement with the change in SAC−CI calculated gas-phase dipole moments upon excitation.